

CdS NANOPARTICLE-DECORATED CuS MICROFLOWER-2D GRAPHENE HYBRIDS AND THEIR ENHANCED PHOTOCATALYTIC PERFORMANCE

Z. G. LI^{a,*}, B. ZENG^b

^a*College of Mechanical Engineering, Hunan University of Arts and Science, Changde 415000, People's Republic of China*

^b*Hunan Collaborative innovation Center for construction and development of Dongting Lake Ecological Economic Zone, Changde 415000, People's Republic of China*

CdS nanoparticles decorated CuS microflower-2D graphene hybrids (CdS/CuS-MF/G) were synthesized in environmentally friendly route and applied as photocatalysts. Composites were characterized with various techniques to investigate their morphology, structure, and optical properties. Photocatalytic activity of samples was evaluated by methyl orange (MO) degradation, and the sample reached photocatalytic efficiency of 84.8% in 120 min. The cause of enhanced photocatalytic activity was attributed to heterojunction in CuS/CdS and excellent electronic conductivity of graphene, which formed three-level electron transfer process. This results in enhanced photogenerated charge carrier separation in composites. Due to high photocatalytic efficiency, as-prepared photocatalyst could encourage further development regarding its application in photocatalytic water treatment.

(Received October 3, 2020; Accepted January 25, 2021)

Keywords: Graphene, Hetero-junction, Photocatalytic

1. Introduction

Due to the potential to degrade environmental pollutants in an environmentally friendly way, heterogeneous photocatalysis has attracted considerable attention in recent years^[1-2]. Metal chalcogenides are promising candidates to be used as photocatalysts, since they possess excellent catalytic activity. Due to the narrow band gap of CuS (2.08 eV), it can absorb photons in the full UV and visible light spectra. Until now, CuS nanostructures with various shapes (nanospheres, nanoplates, nanoflowers, etc.) have been extensively investigated^[3-5]. With respect to the integration of nanoplates into three-dimensional (3D) architectures, microflower have maintained the advantage of nanoplates, as well as achieved some unique properties as a hierarchical assembly^[6]. For instance, Zhao et al. synthesized a rose-like CuS via solvothermal method and they measured excellent photocatalytic activity during the degradation of dyes^[7]. Tanveer et al. prepared CuS microflowers by a sonochemical process which also proved to be highly efficient in the photocatalytic degradation of dyes^[8]. The high photocatalytic activity was attributed to the flower-like morphology, which increased the life span of photogenerated charge carriers and utilized the sunlight efficiently^[9]. However, the photocatalytic activity of CuS by itself is rather limited due to the fast recombination of photogenerated charge carriers^[10]. Therefore, developing strategies to promote the effective photogenerated charge separation of CuS is of great importance.

With the suitable band gap of 2.4 eV, CdS is another popular photocatalytic nanomaterial^[11]. Coupling CdS nanoparticles with other materials to form heterojunction structures is an effective method to promote the effective separation of photogenerated electron-hole pairs and achieve high photocatalytic activity^[12-13]. Therefore, it is reasonable to deduce that constructing CdS-CuS heterojunction could result in enhanced photocatalytic performance.

* Corresponding author: 676747495@qq.com

<https://doi.org/10.15251/CL.2021.181.39>

Graphene-based materials can trap electrons due to their unique electronic properties, making them suitable to enhance the charge separation efficiency in composites^[14-15]. Thus, synthesizing CdS-CuS-graphene systems with unique electronic properties are very promising.

In this work, CdS nanoparticle/CuS microflower/graphene systems were fabricated via a facile microwave method and their photocatalytic performance was investigated. In the composites the heterojunction was formed by decorating CuS microflowers with CdS nanoparticles, while graphene was in direct contact with both of them. Thus, due to the three-level electron transfer process in the composites the separation of photogenerated electron-holes pairs was facilitated.

2. Experimental details

2.1. Synthesis

Typically, 0.05 g of graphene oxide, 4 mmol of copper acetate ($\text{Cu}(\text{AC})_2 \cdot \text{H}_2\text{O}$, $\geq 99.95\%$ purity, Aladdin), 4 mmol of cadmium acetate dihydrate ($\text{Cd}(\text{AC})_2 \cdot 2\text{H}_2\text{O}$, $\geq 99.99\%$ purity, Aladdin), 5 mmol of thioacetamide ($\text{C}_2\text{H}_5\text{NS}$, $\geq 99.9\%$ purity, Aladdin), and 2 g of L-histidine ($\text{C}_{14}\text{H}_{15}\text{N}_3\text{O}_4$, $\geq 99\%$, Aladdin) were added successively into 80 mL of deionized water and was constantly stirred for 30 min. After that, the solution was transferred into a microwave chemical reactor (MCR-3) and was kept at 180 °C for 30 min. Subsequently, the precipitates were filtered and washed with ethanol three times. Finally, the samples were obtained at 60 °C after 12 hours and labeled as CdS/CuS-MF/G. For comparison, a CdS/graphene (CdS/G) sample was also prepared similarly to the as-detailed method without the addition of $\text{Cu}(\text{AC})_2 \cdot \text{H}_2\text{O}$. CuS microflower/graphene (CuS-MF/G) were also obtained using the same method without the addition of $\text{Cd}(\text{AC})_2 \cdot 2\text{H}_2\text{O}$.

2.2. Characterization

X-ray diffraction (XRD) measurements using Cu K α radiation ($\lambda = 0.15406$ nm) were carried out with a Siemens/Bruker D5000 diffractometer. Morphology of the samples was observed by scanning electron microscopy (SEM, Hitachi S-4800) and transmission electron microscopy (TEM, JEM-2100F). The elementary composition was investigated by energy dispersive X-ray spectroscopy (EDS) during the TEM measurements. The diffuse reflectance spectra were recorded with a UV-2500 spectrophotometer. X-ray photoelectron spectroscopy (XPS) measurements were carried out with a K-Alpha 1063 spectrometer employing Al K α X-ray radiation.

2.3. Determination of the photocatalytic performance

Photocatalytic activity of the samples was investigated by the degradation of methyl orange (MO). 30 mg sample was suspended in 500 mL of MO aqueous solution (10 mg/L). Then, the mixture was stirred in dark for 30 min to reach the adsorption/desorption equilibrium of MO. The photocatalytic activity measurements were carried out under visible light irradiation, during which samples were taken every 20 minutes, then they were centrifuged to separate the suspended solid. Then, the concentration of MO was measured by UV-vis spectroscopy at $\lambda_{\text{abs}} = 464$ nm.

3. Results and discussion

Crystalline phase of the CdS/G, CuS-MF/G, CdS/CuS-MF/G samples was determined by XRD measurements. Fig. 1 shows that the main diffraction peaks of CuS-MF/G can be observed at 27.7°, 29.3°, 31.8°, 32.7°, 38.8°, 48.0°, 52.7°, and 59.4° 2 θ values, which were attributed to the (101), (102), (103), (006), (105), (110), (108), and (116) crystal planes of hexagonal CuS (according to the JCPDS No. 06-0460), respectively. In the case of the CdS/G sample the main diffraction peaks can be observed at 26.6°, 28.5°, 43.8°, 47.7°, and 52.1° 2 θ values, which were attributed to the (002), (110), (102), (103), and (012) crystal planes of hexagonal CdS (according to the JCPDS No. 41-1049), respectively. In the case of the CdS/CuS-MF/G sample the observed XRD diffraction peaks at 29.2°, 31.7° and 58.8° could be attributed to the (102), (103), and (116)

crystal planes of CuS (according to the JCPDS No. 06-0460), respectively, while the diffraction peaks at 27.2°, 43.7°, 48.0°, and 51.9° could be attributed to the (101), (110), (103), (012) crystal planes of CdS (according to the JCPDS No. 41-1049), respectively. This implies that well crystallized CuS and CdS nanostructures were present in the samples. Moreover, no obvious characteristic carbon-related diffraction peak could be observed most probably due to the low amount of graphene in the composites^[16].

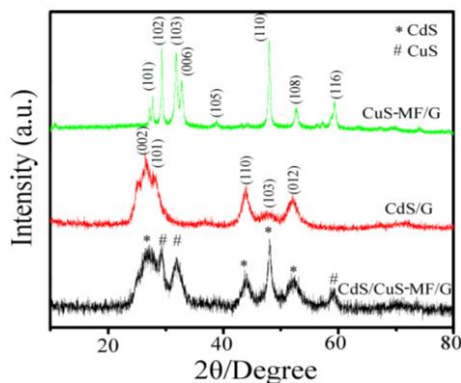


Fig. 1. XRD of the samples.

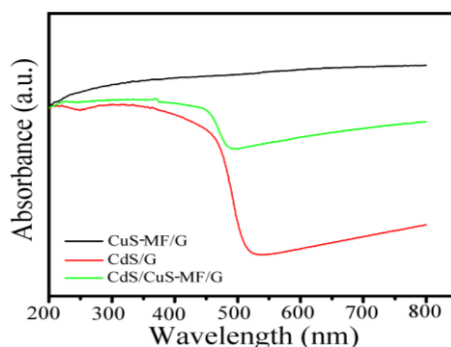


Fig. 2. UV-visible spectra of the samples.

Fig. 2 showed the diffuse reflectance UV-vis spectra for the CdS/G, CuS-MF/G, and CdS/CuS-MF/G samples. The optical absorption edges were estimated to be about 545 nm for CdS/G, and >800 nm for CuS-MF/G. Compared with CdS/G, CdS/CuS-MF/G underwent an obvious red-shift, thus showed increased absorption in the visible light region. Due to the fact that the absorption of CdS/CuS-MF/G was in the visible and NIR region, it could be expected that it possessed significant photocatalytic activity under visible light irradiation^[17].

XPS measurements were carried out to analyze the composition and electronic structure of the materials. Survey spectrum of CdS/CuS-MF/G (Fig. 3a) confirmed the presence of Cd, S, Cu, and C in the sample. As shown in Fig. 3b, a double peak was located at 404.1 and 411.6 eV, which were ascribed to the 3d_{5/2} and 3d_{3/2} transitions of Cd²⁺ in CdS, respectively^[18]. The observed peaks at 935.6 and 955.6 eV were attributed to the Cu²⁺ 2p_{3/2} and 2p_{1/2} binding energies in CuS and the satellite peaks at 943.8 eV and 963.1 eV are also indexed to Cu²⁺ ions, indicating the paramagnetic chemical state of Cu²⁺ ion^[18]. The peaks at 162.5 and 168.5 eV in Fig. 3c are characteristic of S²⁻ in CuS and CdS. In the C1s spectrum, the peaks, the main one centered at 284.8 eV binding energy, were attributed to graphitic sp² carbon (C-C). The drastic decrease of the oxygenated functional groups (286.3 eV, (C-O) and 288.6 eV (O-C=O)) indicated the effective reduction of graphene oxides into graphene and that efficient electron transport ability was achieved in the nanocomposites^[18].

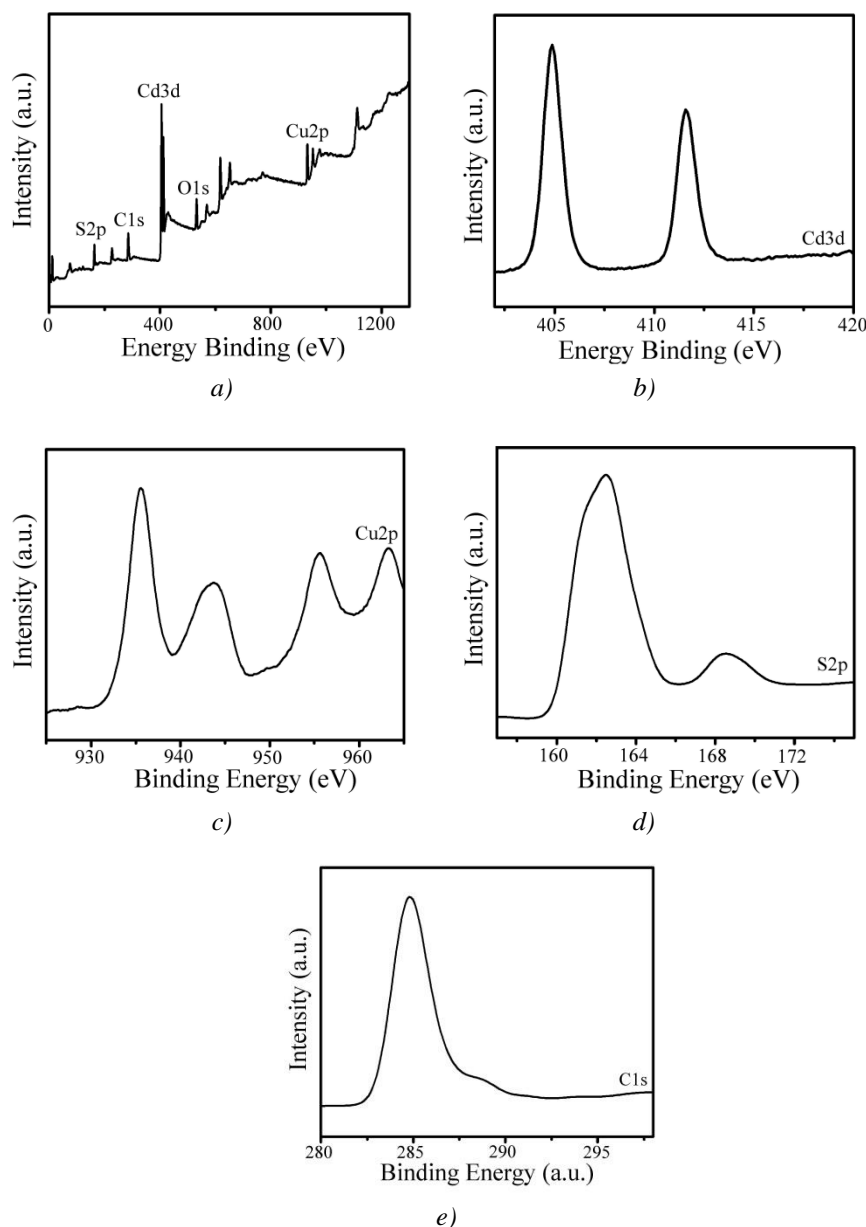


Fig. 3. Typical XPS spectra of the CdS/CuS-MF/G composite: (a) survey spectra, (b) Cd 3d region XPS spectrum, (c) Cu 2 p region XPS spectrum, (d) S2p region XPS spectrum, (e) C1s region XPS spectrum.

As the next step, SEM and TEM measurements were carried out. Based on the SEM measurement (Fig. 4a) CdS/G had spherical shape with ~100-200 nm diameters, and the TEM image (Fig. 4b) showed that these nanospheres were actually formed by the agglomeration of small nanocrystals. The SEM (Fig. 4c) and TEM (Fig. 4d) images for CuS-MF/G both confirmed the 3-dimensional sharp-edged microflower-like structure. Based on the SEM micrograph of sample CdS/CuS-MF/G (Fig. 4e), it had almost the same flower-like structure as CuS-MF/G, however, there were a large amount of nanocrystals attached onto the surface of the petals. Based on the TEM image of the same sample (Fig. 4f) well-defined microflower morphology with the typical nanosheets was observed decorated with numerous nanoparticles. The enlarged TEM image (Fig. 4g) further confirmed the existence of CdS nanoparticles deposited on the surface of CuS nanosheets and it proved that an intimate contact was present between the CdS nanopartilces and CuS nanosheets. Furthermore, the CdS nanopartilces, CuS nanosheets and 2D graphene could be clearly distinguished. The high-resolution transmission electron microscopy (HRTEM) image (Fig. 4g) shows CdS nanoparticles distributed on CuS nanosheets with diameters about 10 nm. The

lattice spacing of 0.188 nm corresponds to the (110) plane of CuS, while 0.33 nm corresponds to the (002) plane of CdS^[19].

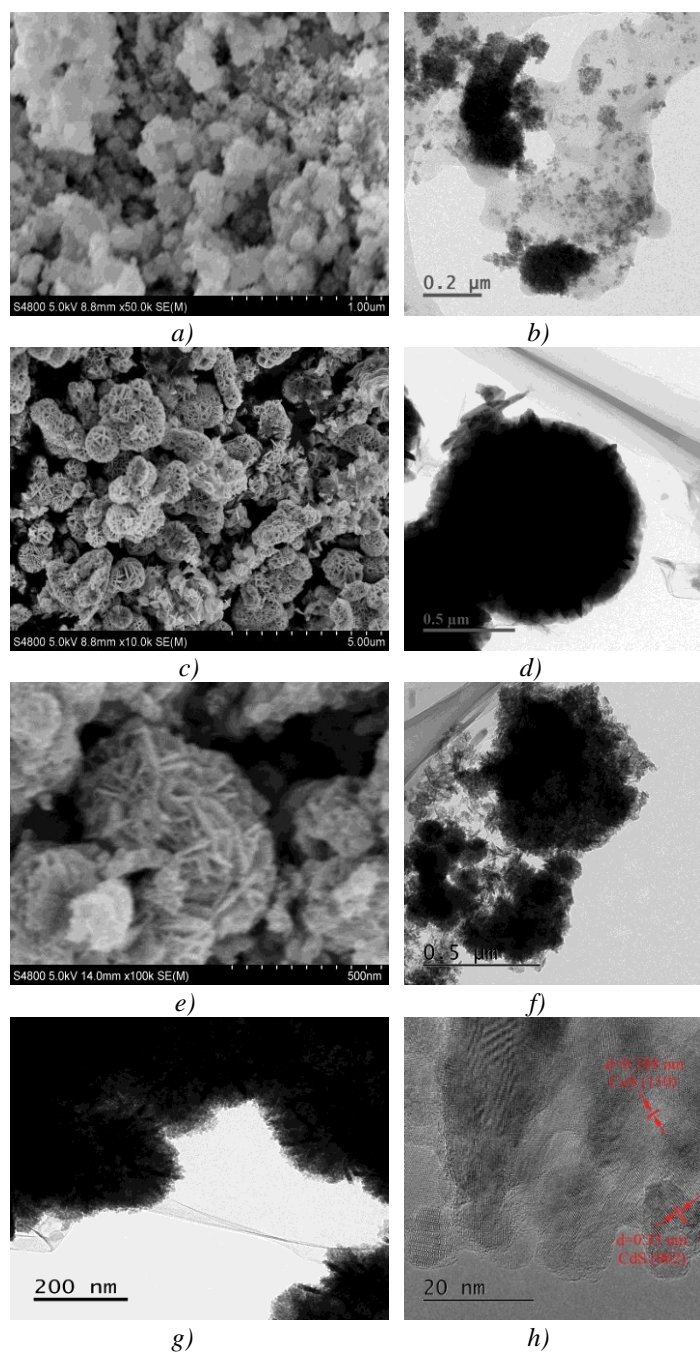


Fig. 4. (a)SEM, (b)TEM of CdS/G, (c)SEM, (d) TEM of CuS MF/G, (e) SEM, (f)(g) TEM, (h) HRTEM of CdS/CuS-MF/G.

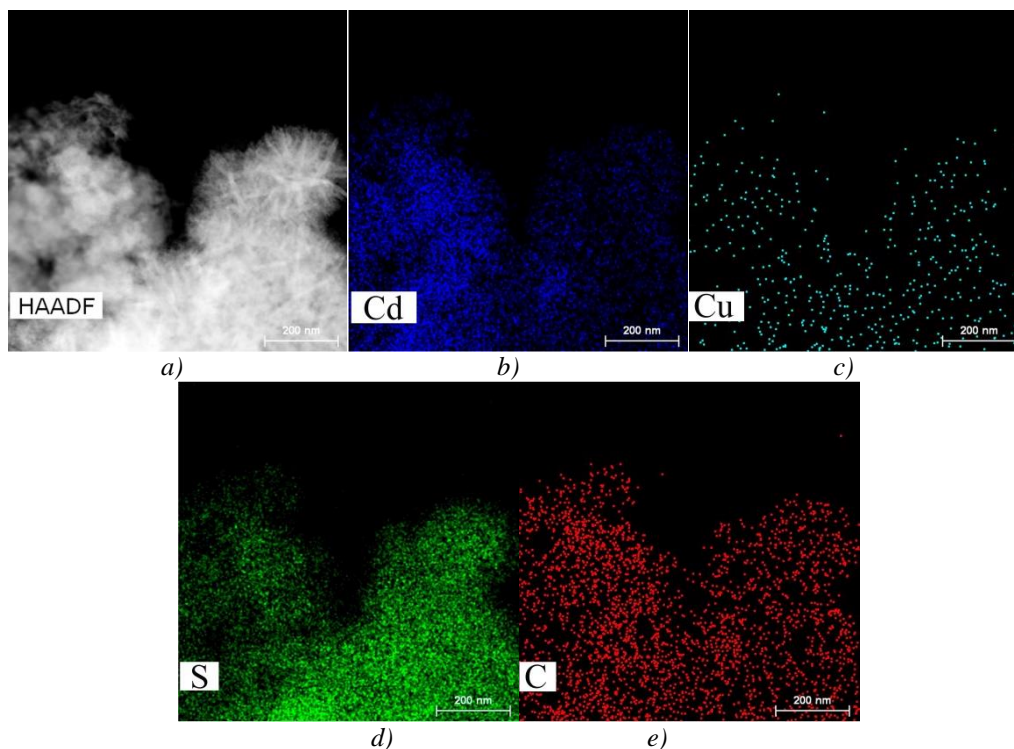


Fig. 5. (a) TEM of EDS mapping of selected area, (b) element Cd mapping, (c) element Cu mapping, (d) element S mapping, (e) element C mapping of CdS/CuS-MF/G.

The elemental composition of CdS/CuS-MF/G was also investigated by EDS measurements and the corresponding element maps. As shown in Fig. 5a, for the EDX elemental mapping analysis such an image was selected where the microflower structure decorated with nanoparticles can be clearly seen. The measurement confirmed the presence of Cd, Cu, S and C in the nanocomposites, further reinforcing the successful addition of CdS and graphene onto the CuS microflowers.

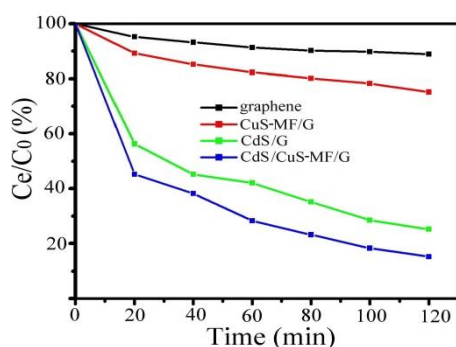
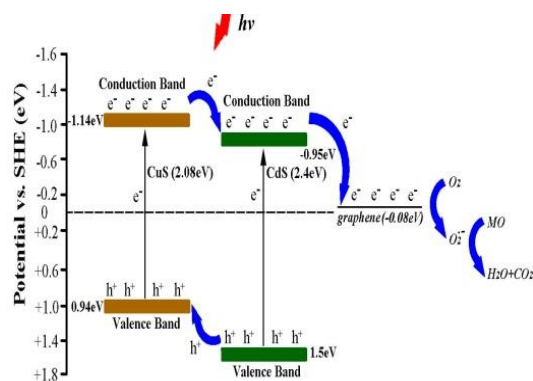


Fig. 6. Photocatalytic degradation efficiency of MO with different catalysts under visible light.

The photocatalytic activity of the samples was investigated via the degradation of MO under visible irradiation and the results are shown in Fig. 6. The photodegradation of MO by graphene was negligible, and in the case of CuS-MF/G only 24.8% degradation was observed, indicating the easy electron-hole recombination in CuS. For CdS/G the degraded amount of MO increased up to 74.8% due to its suitable band gap. In the case of CdS/CuS-MF/G, the even higher photocatalytic efficiency (84.8%) was achieved.



Scheme 1. Schematic illustration for the charge transfer and separation in the CdS/CuS-MF/G.

To explain the cause of the observed photocatalytic activities, a plausible mechanism was proposed in Scheme 1. Initially, CuS absorbed visible light and generated electron-hole pairs, however, their rapid recombination lead to low photocatalytic efficiency^[20]. However, the presence of CdS nanoparticles on the CuS nanosheets could result in the formation of a heterojunction, which could favor the separation of electron-hole pairs (the photogenerated-electrons are transferred from CuS to CdS in the conduction band and photogenerated-holes are transferred from CdS to CuS in the valence band)^[20]. Furthermore, when graphene was added to the CdS/CuS system, it served as an excellent electron transport matrix that can capture photoelectrons, thus avoiding electron-hole recombination resulting in efficient electron-hole separation. Therefore, the photocatalytic activity of the G/CuS/CdS system was gradually increased by assembling heterojunction with graphene nanosheets^[20]. Consequently, more electrons were transferred to graphene and then these electrons reduced O_2 into superoxide radical, which degraded MO directly.

4. Conclusions

In summary, CdS nanoparticle-decorated CuS microflower-2D graphene hybrids were successfully constructed via a microwave method. In this sample, graphene and the CdS/CuS-MF system had well-matched band gap energies and formed efficient three-level electron transfer within the composite, which facilitated the efficient charge separation upon visible light irradiation, resulting in excellent photocatalytic activity. Hopefully, the presented facile synthesis strategy can promote the environmental application of this system.

Acknowledgments

This work was supported by the Project of Hunan Provincial Education Department(19A341) and the project of Hunan Provincial Natural Science Foundation of China (2020JJ6006).

References

- [1] X. Y. Liu, C. S. Chen. *Mater. Lett.* **261**, 127127 (2020).
- [2] C. S. Chen, X. Y. Liu, Q. Fang et al., *Vacuum* **174**, 109198 (2020).
- [3] R. Rameshbabu, P. Ravi, M. Sathish. *Chem. Eng. J* **360**, 1277 (2019).
- [4] Z. Bano, R. M. Yousaf Saeed, S. Zhu et al. *Chemosphere* **246**, 125846 (2020).
- [5] B. Zeng, W. F. Liu, W. J. Zeng et al., *Nano* **13(3)**, 1850029 (2018).
- [6] Y. F. Fu, Q. Li, *J Colloid Interf. Sci.* **570(15)**, 143 (2020).

- [7] L. J. Zhao, L. Zhou, C. C. Sun et al., *Cryst. Eng. Comm.* **20**, 6529 (2018).
- [8] M. Tanveer, C. B. Cao, I. Aslam et al., *New J. Chem.* **39**, 1459 (2015).
- [9] T. W. Cai, Y. Ding. *Func.Mater. Lett.* **12**(2), 1590002 (2019).
- [10] B. Zeng, W. F. Liu, W. J. Zeng et al. *J. Nanopart. Res.* **20**, 55 (2018).
- [11] B. Zeng, W. F. Liu, W. J. Zeng et al., *J. Mater. Sci. Mater-El.* **30**, 3753 (2019).
- [12] M. A. Pandit, S. Billakanti, K. Muralidharan. *J. Environ. Chem. Eng.* **8**(2), 103542 (2020).
- [13] L. F. Luo, Y. D. Wang, S. P. Huo et al. *Inter. J. Hydrogen Energy* **44**(59), 30965 (2019).
- [14] C. S. Chen, S. Y. Cao, H. Long et al., *J. Mater. Sci-Mate. El.* **26**, 3385 (2015).
- [15] C. S. Chen, W. W. Yu, T. G. Liu et al., *Sol. Energ. Mat. Sol. C* **160**, 43 (2017).
- [16] W. J. Ren, H. W. Chang, T. Y. Mao et al., *Chem. Engin. J* **362**, 160 (2019).
- [17] J. H. Duan, X. K. Song, H. Zhao et al., *Opt. Mater.* **101**,109761 (2020).
- [18] B. Zeng, W. J. Zeng, *J. Nanosci. Nanotech.* **20**, 17201 (2020).
- [19] F. Zhang, H. Q. Zhuang, W. M. Zhang et al., *Catal. Today* **330**(15), 203 (2019).
- [20] X. L. Deng, C. G. Wang, H. C. Yang et al., *Scientific Rep.* **20**, 3877 (2017).